Supplementary information

Correspondence and requests for materials should be addressed to
H.E. (hermann.ehrlich@physik.tu-freiberg.de)

Discovery of 505-million-year old chitin in the basal demosponge *Vauxia gracilenta*

H. Ehrlich[1*], J. Keith Rigby[2§], J. P. Botting[3], M. V. Tsurkan[4], C. Werner[4], P. Schwille[5], Z. Petrášek[5], A. Pisera[6], P. Simon[7], V. N. Sivkov[8], D. V. Vyalikh[9], S. L. Molodtsov[1,10], D. Kurek[11], M. Kammer[12], S. Hunoldt[12], R. Born[13], D. Stawski[14], A. Steinhof[15], V. V. Bazhenov[1], and T. Geisler[16]

[1] Institute of Experimental Physics, TU Bergakademie Freiberg, D-09599 Freiberg, Germany

[2] Museum of Paleontology, Brigham Young University, Provo, Utah, USA 84602-3300

[3] Leeds Museum Discovery Centre, Leeds LS10 1LB, UK

[4] Leibniz Institute of Polymer Research Dresden, Max Bergmann Center of Biomaterials, D-01069 Dresden, Germany

[5] Max Planck Institute of Biochemistry, 82152 Martinsried, Germany

[6] Institute of Paleobiology, Polish Academy of Sciences, 00-818 Warszawa, Poland

[7] Max Planck Institute of Chemical Physics of Solids, D-01187 Dresden, Germany

[8] Department of Mathematics Komi SC UrD RAS, Syktyvkar, Russia

[9] Institute of the Solid State Physics, Dresden University of Technology, D-01069 Dresden, Germany

[10] European XFEL GmbH, Albert-Einstein-Ring 19, D-22761 Hamburg, Germany

[11] Centre “Bioengineering”, Russian Academy of Sciences, 117312 Moscow, Russia

[12] Institute of Bioanalytical Chemistry, TU Dresden, D-01069 Dresden, Germany

[13] R&D Chemistry, EKF Diagnostics, D-39179 Barleben, Germany

[14] Department of Material Commodity Sciences and Textile Metrology, Lodz University of Technology, 90-924 Łódź, Poland

[15] Max Planck Institute of Biogeochemistry, D-07701, Jena, Germany

[16] Steinmann-Institut für Geologie, Mineralogie und Paläontologie, University of Bonn, D-53115 Bonn, Germany

[§] Deceased

Methods and Text

Transmission electron microscopy (TEM). TEM images and electron diffraction were recorded by a FEI Tecnai 10 equipped with LaB_6-source and at 100 kV acceleration voltage. Micrographs were recorded by means of TEM camera F224HD 2k x 2k (TVIPS company, Gauting, Germany) with an active area of 49 mm x 49 mm and a dynamic range of 25 000:1. For electron microscopy, a drop of the water suspension containing the sample was placed on the electron microscopy grid (Plano GmbH, Wetzlar, Germany) covered with a perforated carbon film. The sample thereafter was dried in air.

Scanning electron microscopy (SEM). For the SEM experiments, the samples were fixed on a sample holder and the surface was covered with carbon for 1 min using an Edwards S150B sputter coater. The samples were then placed in an LEO DSM 982 Gemini scanning electron microscope. SEM investigations presented in Fig. S9 were performed by means of an ESEM FEI Quanta 200 FEGi system with a field emission gung operated in high vacuum mode and at an acceleration voltage of 15 kV (FEI company, Eindhoven, NL). Energy dispersive X-ray microanalysis (EDX) was carried out using this instrument.

Staining and detection of chitin.
To elucidate the particular location of chitin in investigated samples, we used Calcofluor White (Fluorescent Brightener M2R, Sigma). Samples were placed in 0.1 M Tris-HCl at pH 8.5 for 30 minutes, then stained using 0.1% (w/w) Calcofluor White solution for 30 minutes in darkness, rinsed five times with deionized water, dried at room temperature, and finally observed using fluorescence microscopy (Keyence BZ-8000K).

Chitinase digestion.
Chitinase (EC 3.2.1.14, No. C-8241, Sigma) from the fungus *Trichoderma viride* was used. The sample (Fig. S8) was incubated with chitinase dissolved in 0.2 M citrate phosphate buffer at pH 4.5 at 25 C or in the buffer as a control. Enzyme solutions were made in the same buffer with concentrations of 0.5 mg/ml. The effectiveness of the enzymatic digestion was monitored using optical microscopy (Zeis, Axiovert).

Identification of D-glucosamine.
Sample preparation.
The organic matrix fragments obtained after HF-treatment of fossil sponge samples were hydrolyzed in 6 M HCl for 24 hours at 37°C. Hydrolyzed samples were filtered with a 0.4 micron filter and freeze dried in order to remove the excess of HCl. The solid remains were split in half. One half was dissolved in ddH_2O for chromatography and electrophoresis analyses, and the other dissolved in MeOH for ESI-MS analysis. The standard D-glucosamine was purchased from Sigma (USA).

High performance liquid chromatography (HPLC).
HPLC experiments were performed by analytical HPLC XBridge BEH 300 C-18 column (5μM particle size, 2.1×250 mm, Waters, USA) over 40 min using the flow rate of 0.5 ml/min for the analytical column. A linear gradient of water/acetonitrile containing 0.1 % (v/v) trifluoroacetic acid was used as the mobile phase *(1)*. For HPLC separations, the monitoring wavelengths were set a wavelength range of 210-

278 nm. A two-pump system (Agilent Technologies 1200 Series) equipped with a UV/Vis detector/spectrophotometer having a 1 cm path length cell was used.

High performance size exclusion chromatography (HPSEC).
HPSEC experiments were performed on BioSep-SEC-S 2000 column (Phenomenex, USA) The peptide samples were eluted using 50 mM KH_2PO_4/ 100 mM KCl, pH7, with 0.2-0.5 ml/min flaw rate, and monitored at a wavelength range of 210-278 nm *(2, 3)*. To keep reproducibility of the results, purification of the columns using DMSO was performed after every 20-30 runs. A two-pump system (Agilent Technologies 1200 Series) equipped with a UV/Vis detector/spectrophotometer having a 1-cm path length cell was used.

High performance capillary electrophoresis (HPCE).
The experiment was performed at positive polarity on silica capillary with 60 cm length (Beckman, CA, USA). The separations were run under a constant voltage of 30 kV and the detection was set at a wavelength range of 190-300 nm. A 100 mM Sodium borate buffer, pH 8.3, was used for electrophoretic separation *(4)*. The samples were injected for 5 second under 0.5 psi pressure. To keep reproducibility of the results, the capillary was washed between each run with 0.1 M NaOH and then water, followed by reconditioning with the running buffer. A Beckman PA800 CE system (Fullerton, CA, USA) equipped with PDA detector was used.

Electrospray ionization mass spectrometry (ESI-MS).
All ESI-MS measurements were performed on Mariner spectrometer (Applied Biosystems, USA) equipped with a syringe pump. Nitrogen was used as the nebulizing and dessolvation gas.

Thermogravimetric analysis (TGA).
TGA studies were performed using a Perkin Elmer TGA 7 apparatus in flowing nitrogen (20 cm^3/min), at a heating rate of 10 ^oC/min in a platinum measuring cell. Each measurement was repeated at least three times.

C^{14} analysis of possible modern contamination.
A fossil sample was cleaned, ground and sieved (63 µm mesh size). The carbon contents were measured with an elemental analyzer (NC2500, Carlo Erba Instruments, Milan, Italy) coupled to a mass spectrometer (Delta Plus, Thermo Quest, Bremen, Germany). After the HCl treatment the sample was split. A part was washed for 6 h in a saturated $Na_4P_2O_7$ solution with 0.5 M NaOH. The solution was exchanged every hour. Afterwards the sample was washed three times with water and three times for 1 hour with 2 M H_2SO_4. A second part of the sample was washed 3 times for 1 hour with 10 % $KClO_3$ in 35% HNO_3. The sample then were freeze dried and graphitized (*28*). The carbon contents of both sample parts were changed by less than 0.5 % (within an uncertainty of 10%). The AMS measurements were performed at the Jena AMS system (*29*).

Calcofluor White Staining of chitinous *Ianthella basta* sponge skeleton after 300°C treatment.
Ianthella basta (Verongida: Demospongiae: Porifera) sponge skeleton possess 5% (weight) of chitin (*30*). Cells and tissue-free chitinous skeleton were thermally treated in purified marine sand for 12 hours at 300°C in an argon atmosphere.

After this procedure, dark-colored skeletal fibers were incubated for 1 h at room temperature in 3 M HCl as well as in 48 % HF for removing residual sand microparticles.

After that, samples were rinsed four times in deionized water, dried at 50 °C and stained using Calcofluor White (CFW) for identification of chitin as described by us previously (*31*).

Supplementary results

FTIR analysis.

Results of the FTIR investigations on the fragments of organic matrix isolated from fossilized *V. gracilenta* after HF-based treatment and represented in Fig. S6.

Sample A

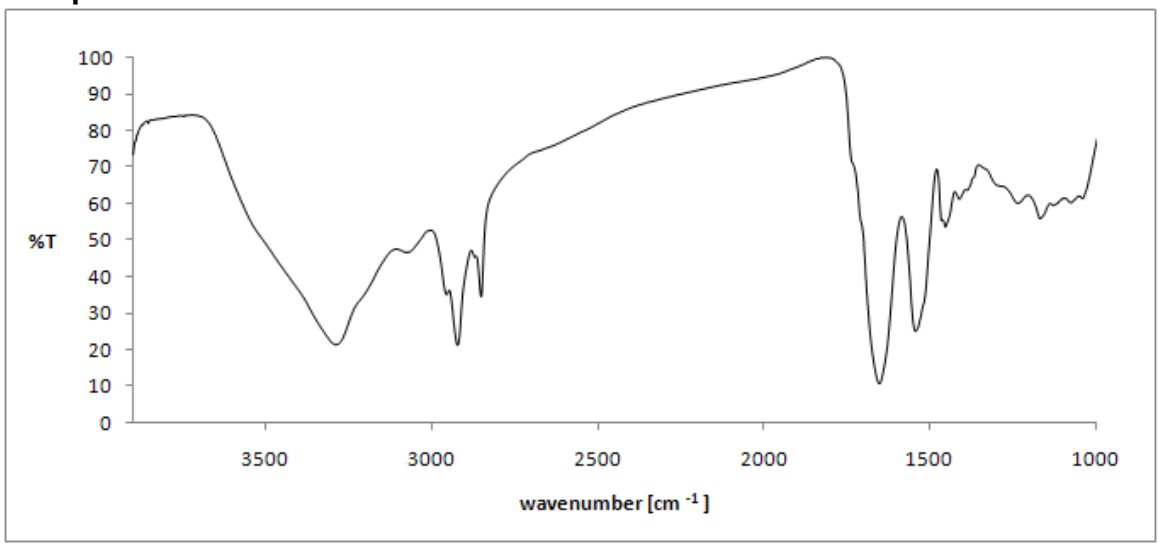

α-chitin Standard	Sample A	Assignment	References
3265	3289	NH symmetric and asymmetrical stretching vibration	*5,6,7*
2965	2956	C-H stretching (pyranose ring) / CH_3 stretching	*5, 7, 8, 9, 10*
2932	2922	C-H stretching (chitin), (ν ($COCH_3$))	*5, 8, 10, 11, 12*
2877	2869	CH_2 stretching (pyranose ring)/C-H stretching	*5, 10*
	2852	CH_2 stretching (pyranose ring)/C-H stretching	*5*
1658	1653	Amide I band	*5, 7, 8, 9, 10,11, 12*
1556	1545	Amide II band	*5, 7, 10*
1466	1466	CH_2 bending (pyranose ring)	*5*
	1454	CH_2 bending	*5*
	1413	CH_2 bending and CH_3 deformation	*5*
1156	1170	Pyranose C-C, C-O stretching/asym brigde oxygen stretching	*5, 8*
1072	1078	C-O stretching	*5, 6, 8, 9, 10*

Sample B

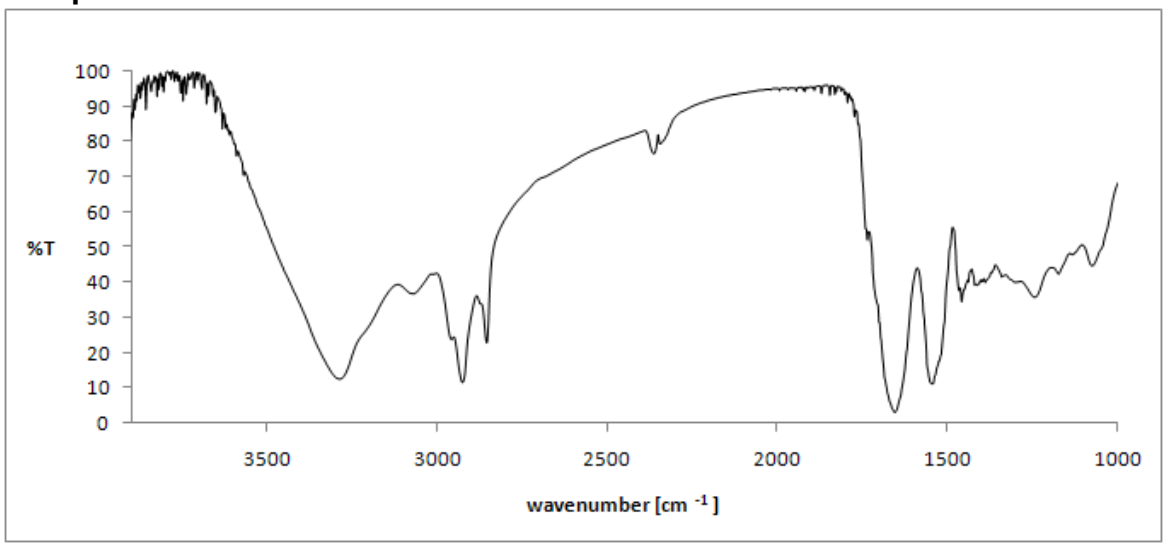

α-chitin Standard	Sample B	Assignment	References
3265	3284	NH symmetric and asymmetrical stretching vibration	*5,6,7*
2965	2956	C-H stretching (pyranose ring) / CH_3 stretching	*5, 7, 8, 9, 10*
2932	2924	C-H stretching (chitin), (ν ($COCH_3$))	*5, 8, 10, 11, 12*
2877	2871	CH_2 stretching (pyranose ring)/C-H stretching	*5, 10*
	2852	CH_2 stretching (pyranose ring)/C-H stretching	*5*
1658	1654	Amide I band	*5, 7, 8, 9, 10,11, 12*
1556	1554	Amide II band	*5, 7, 10*
1466	1464	CH_2 bending (pyranose ring)	*5*
	1457	CH_2 bending	*5*
	1411	CH_2 bending and CH_3 deformation	*5*
1156	1172	Pyranose C-C, C-O stretching/asym brigde oxygen stretching	*5, 8*
1072	1074	C-O stretching	*5, 6, 8, 9, 10*

Sample C

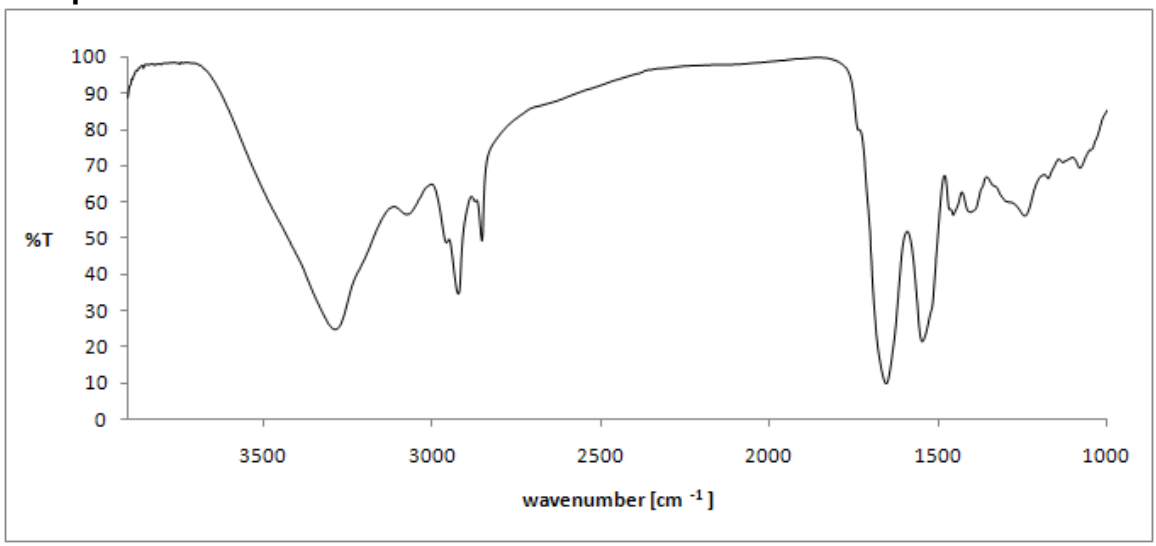

α-chitin Standard	Sample C	Assignment	References
3265	3284	NH symmetric and asymmetrical stretching vibration	*5,6,7*
2965	2956	C-H stretching (pyranose ring) / CH_3 stretching	*5, 7, 8, 9, 10*
2932	2923	C-H stretching (chitin), (ν ($COCH_3$))	*5, 8, 10, 11, 12*
2877	2871	CH_2 stretching (pyranose ring)/C-H stretching	*5, 10*
	2850	CH_2 stretching (pyranose ring)/C-H stretching	*5*
1658	1654	Amide I band	*5, 7, 8, 9, 10,11, 12*
1556	1547	Amide II band	*5, 7, 10*
1466	1466	CH_2 bending (pyranose ring)	*5*
	1454	CH_2 bending	*5*
	1405	CH_2 bending and CH_3 deformation	*5*
1156	1172	Pyranose C-C, C-O stretching/asym brigde oxygen stretching	*5, 8*
1072	1078	C-O stretching	*5, 6, 8, 9, 10*

Sample D

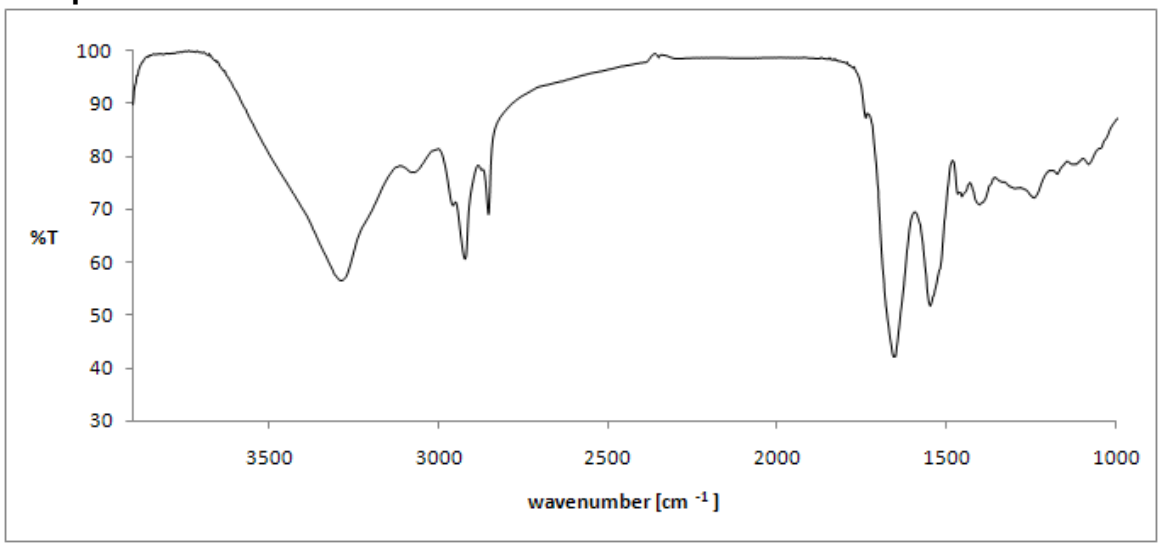

α-chitin Standard	Sample D	Assignment	References
3265	3283	NH symmetric and asymmetrical stretching vibration	*5,6,7*
2965	2956	C-H stretching (pyranose ring) / CH_3 stretching	*5, 7, 8, 9, 10*
2932	2920	C-H stretching (chitin), (ν ($COCH_3$))	*5, 8, 10, 11, 12*
2877	2872	CH_2 stretching (pyranose ring)/C-H stretching	*5, 10*
	2851	CH_2 stretching (pyranose ring)/C-H stretching	*5*
1658	1651	Amide I band	*5, 7, 8, 9, 10,11, 12*
1556	1547	Amide II band	*5, 7, 10*
1466	1466	CH_2 bending (pyranose ring)	*5*
	1454	CH_2 bending	*5*
	1403	CH_2 bending and CH_3 deformation	*5*
1156	1172	Pyranose C-C, C-O stretching/asym brigde oxygen stretching	*5, 8*
1072	1078	C-O stretching	*5, 6, 8, 9, 10*

Identification of D-glucosamine in hydrolyzed fragments of *V. gracilenta* organic matrix.

D-glucosamine (DGlcN) elutes in HPLC, which is set at 210 and 278 nm, as a single peak at 1.73 minutes (Fig. S11). This elution time is only slightly longer than the zero volume of the column which can be seen by the characteristic absorption distortion at 1.5 minutes. The 250 nm was chosen for the monitoring because D-glucosamine does not deposit absorption at this wavelength whereas many possible impurities such as sulfides, terpenes or any aromatic compounds have absorption in this region. The HPLC of the (hydrolyzed) sample showed the presence of one main peak with the similar elution time of 1.73 min. Similar to the standard, the sample does not show any strong absorption at 250 nm. The single peak in the HPLC clearly suggests the similarity in nature of the sample and the standard *(13)*. Nevertheless,

the high hydrophilicity of DGlcN and therefore its short elution time makes the application of HPLC ambiguous in this case.

High performance size exclusion chromatography HPSEC was used as an alternative to the HPLC method. Charged saccharides such as heparin or poly glucosamine have a strong specific interaction with sorbent in HPSEC columns and therefore in many cases is difficult to be separated by size *(14, 15)*. In principle, HPSEC is not a good method for the separation of monosaccharides, but it can distinguish them from many low molecular weight species of different nature.

D-glucosamine elutes as a single peak in HPSEC with an elution time of 21.3 min which can be seen only by monitoring 210 nm absorption (Fig. S12). The sample deposits only one peak at 21.5 minutes which is similar to the elution time of DGlcN. The sample deposits strong absorption at 210 as well as 250 and 278 nm. This result indicates that the sizes of the standard and the sample are comparable but the sample is a mixture of compounds, separation of which by HPSEC was not successful.

HPCE has been shown to be an excellent technique for characterization of monosaccharide derivatives *(16)*. The chemical modification of monosaccharides by 1-phenyl-3-methyl-5-pyrazolone (PMP), 6-aminoquinoline (6-AQ) and so on is necessary for their visualization in UV-Vis spectral region. HPCE of underivatized carbohydrates is not used widely. The reason for that is the limited sensitivity because of the very low absorption of most carbohydrates even in the far UV spectrum. Nevertheless, it has been shown that glycosamines can be detected directly by UV-Vis spectrum under some experiment conditions *(17, 18)*. Among many of them, borate buffer seems to be the most acceptable and allows detection of underivatized glycosamines at up to 214 nm with acceptable sensitivity *(19)*.

In HPCE, DGlcN elutes as a single peak with an elution time of 2.36 min which can be seen by monitoring 210 nm absorption (Fig. S13). The sample reveals several main peaks in HPCE, the largest of which has identical elution time with DGlcN. As it shown in Fig. S13, the UV-Vis spectra of DGlcN and the largest peak of the sample are equivalent. This result clearly indicates that the sample contains a species that is highly similar in its properties to DGlcN. Mass spectroscopy analysis was expected to reveal if this specie is indeed DGlcN.

ESI-MS of D-glucosamine standard shows three signal m/z = 162.06, 180.07 and 359.13. The signal with m/z = 180.07 corresponds to the molecular ions $[M + H^+]$ of a species with a molecular weight 179.07 which is DGlcN (calculated: 179.1). The signal at m/z = 162.06 corresponds to a fragment ion $[M - H_2O + H^+]$ in which DGlcN lost of one water molecule (calculated: 162.1) and is very common for this type of molecules *(20, 21)*. The signal at m/z = 359.13 is corresponded to $[2M + H^+]$ species which is proton-bound DGlcN non covalent dimmer *(21)*.

ESI-MS of the sample has revealed many signals (Fig. S14). Among them the signals of GlcN and its derivatives (m/z = 162.06, 180.07 and 359.13) are detected as the dominant product of the sample hydrolysis. Among many other signals, the species with m/z = 341.12 and 502.17 are common for MS analyses of chitosan hydrolysis products *(22, 23)* and correspond to unhydrolyzed oligosaccharides. In this case the species with m/z = 341.12 corresponds to the disaccharide $[(GlcN)_2 + H^+]$ and m/z = 341.12 trisaccharide $[(GlcN)_3 + H^+]$.

Thermogravimetric investigations of chitin from the sponge *Aplysina aerophoba* (Verongida: Demospongiae: Porifera).

In the first step, the *A. aerophoba* chitinous skeletons (*32*) were analyzed by heating up to 300 ^oC (then the process was stopped) and in full measurements (up to

600 ^{o}C) in both cases without any previous drying or conditionation. The representative TG curve of skeleton thermal degradation is presented below (Fig. S15). Obtained results show that the main degradation process starts at about 345 ^{o}C.

The samples heated to 300 ^{o}C were compared with unheated samples using FTIR spectroscopy. The spectra (Fig. S16) are almost identical. We conclude that there are no significant changes in the primary material of the sponge chitinous skeleton samples under such temperature range even under prompt heating conditions, at least under short timescales. Therefore, we suggest that chitinous skeletons preserved in a mineral envelope, if they were not initially damaged by chitinolytic bacteria, would not be expected to be destroyed under conditions of the low grade methamorphism (near 260°C), which has been developed slowly and during a very long time.

Calcofluor White staining of chitinous *Ianthella basta* sponge skeleton after 300°C treatment.

The fluorescence microscopy images (Fig. S17 and S18) show irregular morphology of the surface of the thermal treated chitinous sponge fibers. These images differ from those obtained for *thermally untreated* chitinous sponge fibers (Fig. S19) where homogenous distribution of the fluorescence can be observed.
Thus, it is possible to confirm the survival of chitin in skeletal fibres of recent Verongida sponges using CFW staining even after thermal treatment under anoxic conditions at 300°C. Obtained results are in a good agreement with data reported above with regard to results of thermogravimetric analysis.

Results of ^{14}C measurements.

Fig. S20 shows the conversion of the measured concentration of the sample treated with $KClO_3$ in calendar years. The age of 43000 ±1200 years BC (1 σ confidence interval) has to be seen as minimum age resulting from contaminations. Several sources of contaminations could be considered: (i) post-sampling bacterial degradation (*33*), (ii) contamination due to infiltration of humic acids from the top soil which couldn't be removed completely (*34*), or (iii) incorporation of modern CO_2 as ferrous carbonate, which cannot be removed by the applied treatments. Each of this contamination processes can lead to much larger faults in age, e.g. process (i) can induce for coal ages starting from 25 kyr (*33*).

Fluorescence microscopy imaging of DNA in *V. gracilenta* fossil

With the aim of determining the possible locality of DNA if preserved in the *Vauxia* fossil samples, we employed fluorescence microscopy together with fluorescent DNA binding dyes. Selected fragments were incubated at room temperature in Bisbenzimide H 33342 (1 mg /ml, Sigma-Aldrich) and SYBR Green I DNA (Product Nr.850512, BIOZYM) dyes for approximately 20 min according to protocol by Oskam et al (2009) (37), then imaged. Stained specimens were imaged using KEYENCE BZ-8000K microscope.
Both staining procedures lead to obtaining of negative results (Fig. S21) with respect to DNA identification in the investigated samples.

DNA extraction from the rock with fossil *V. gracilenta*

We used protocol proposed by Barton et al in 2006 (38) for DNA extraction from the carbonate rock. Our improved extraction protocol also involved 0.5 g of rock sample

that was placed into liquid nitrogen and being crushed in a flamesterilized Ahat pestle and mortar. The crushed material was mixed with 500 µl 2x buffer (200 mM Tris (pH 8.0), 50 mM EDTA, 300 mM EGTA, 200 mM NaCl), to which was added 3 mg/ml lysozyme (L7651, Sigma-Aldrich) and 5 µg poly(dexoyinosinic-deoxycytidylic) acid (P4929, Sigma-Aldrich). The mix was then incubated at 37 °C for 30 min, prior to the addition of Proteinase K from *Tritirachium album* (Roth, Germany) (to 1.2 mg/ml) and sodium dodecyl sulfate (71727 FLUKA, Sigma-Aldrich) (SDS to 0.3% wt/vol) and further incubation at 50 °C for 30 min. SDS was increased to 5% wt/ vol and the samples were disrupted on a mini-bead beater -24 (Biospec) at low speed for 2 min and high speed for 30 s in the presence of 50% (v/v) phenol–chloroform–isoamyl alcohol (25:24:1). The supernatant was collected and extracted with an equal volume of phenol– chloroform–isoamyl alcohol (25:24:1) (38). The supernatant was again removed and 5 µg of poly-dIdC was added before precipitation with 0.5M sodium acetate and 2 volumes of high-grade ethanol followed by centrifugation at 15,000 x g.

No DNA in any detectable form has been observed in the supernatant.

The ESI-MS spectra of the rock samples

The ESI samples of the rock were obtained by scratching the surface of the rock in the close proximately to the *Vauxia gracilenta* sponges remains. The collected rock samples were treated in a similar way to *Vauxia* samples and were hydrolyzed in 6 M HCl at 60 °C for 24 hour. Next, the samples were filtrated and freeze-dried to remove the excess of HCL; the remains were dissolved in methanol right before ESI-MS analysis. The samples of the rock have revealed no strong signals in ESI-MS measurements (Figure S22). The intensity of the signals corresponds to the background noise which appears in the instrument detector when MeOH is used as a solvent. The main signal in the spectra is a specie with MW/z = 149 which is a typical artifact coming from plasticizer. The ESI-MS spectra of pure MeOH (LC-MS grade) is presented in the figure S23 for the reference.

Supporting Figures

Figure S1. **|** Samples from Burgess Shale containing fossilized *Vauxia* specimens. From left to the right: accession number ROM 75-2840; ROM 61-237 and ROM 75-2854,

Figure S2. | Raman scattering of areas of the rock samples with accession numbers ROM 75-2840 (a); ROM 61-237 (b) and ROM 75-2854 (c) (Fig. S1) revealed vibrational bands characteristic of carbonaceous materials at about 1300 cm^{-1} and 1590 cm^{-1}, which are commonly designated D (disordered) and G (ordered or graphitic), respectively. All of the samples show similar origin with respect to thermal low-grade metamorphism.

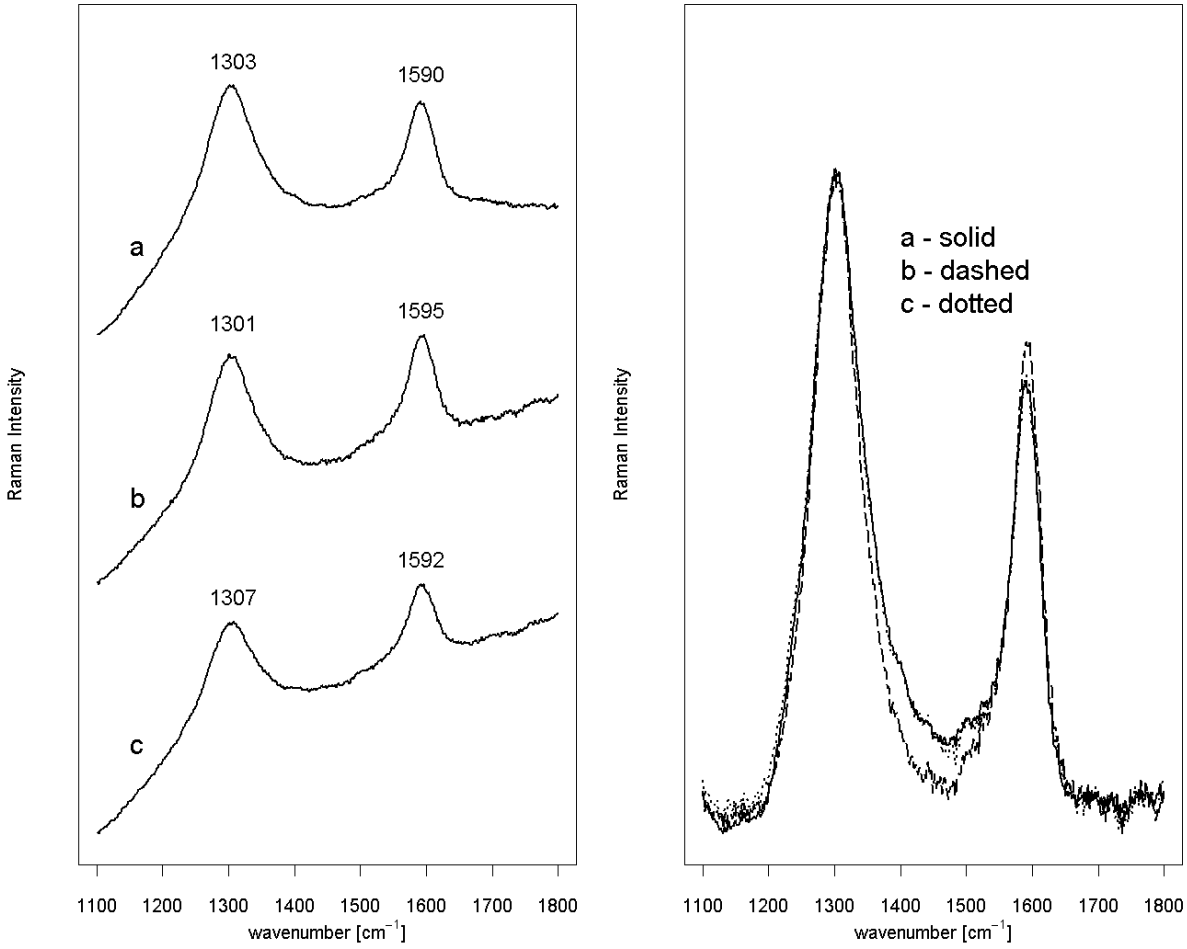

Figure S3. | Overview: initial cleaning of the specimen surface using Osteosoft (Merck) solution which contains 177 g/L of EDTA, pH 7.3.

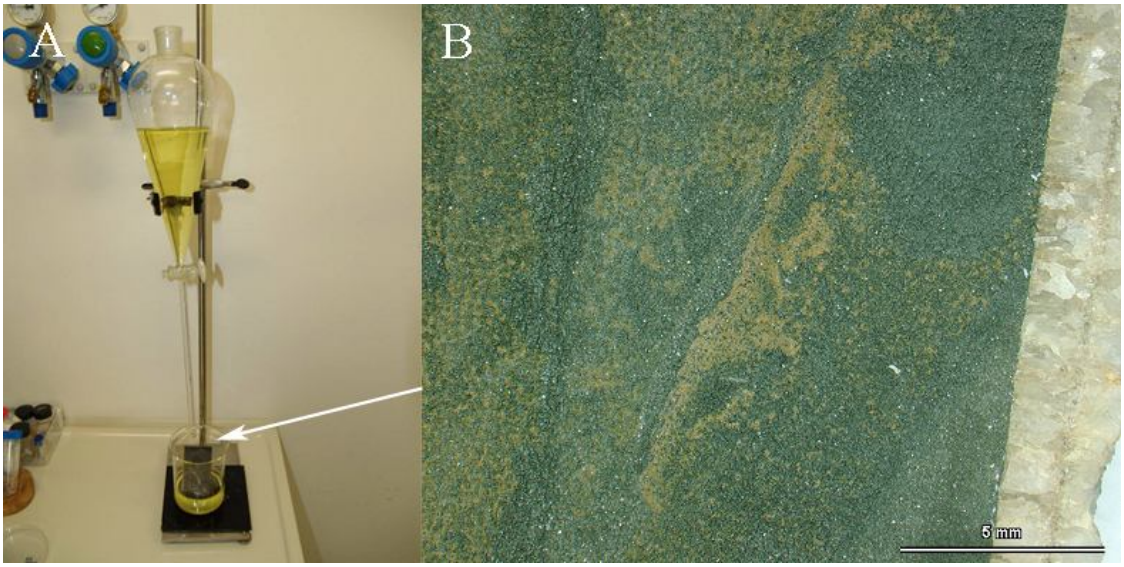

Figure S4. | Calcofluor White staining of the surface of the preliminarily cleaned rock with fossilized *V. gracilenta* leads to visualization of preserved chitinous material (A). Fragments of similar shape, size and morphology are observed also using SEM (B) after HF-based treatment of the sample.

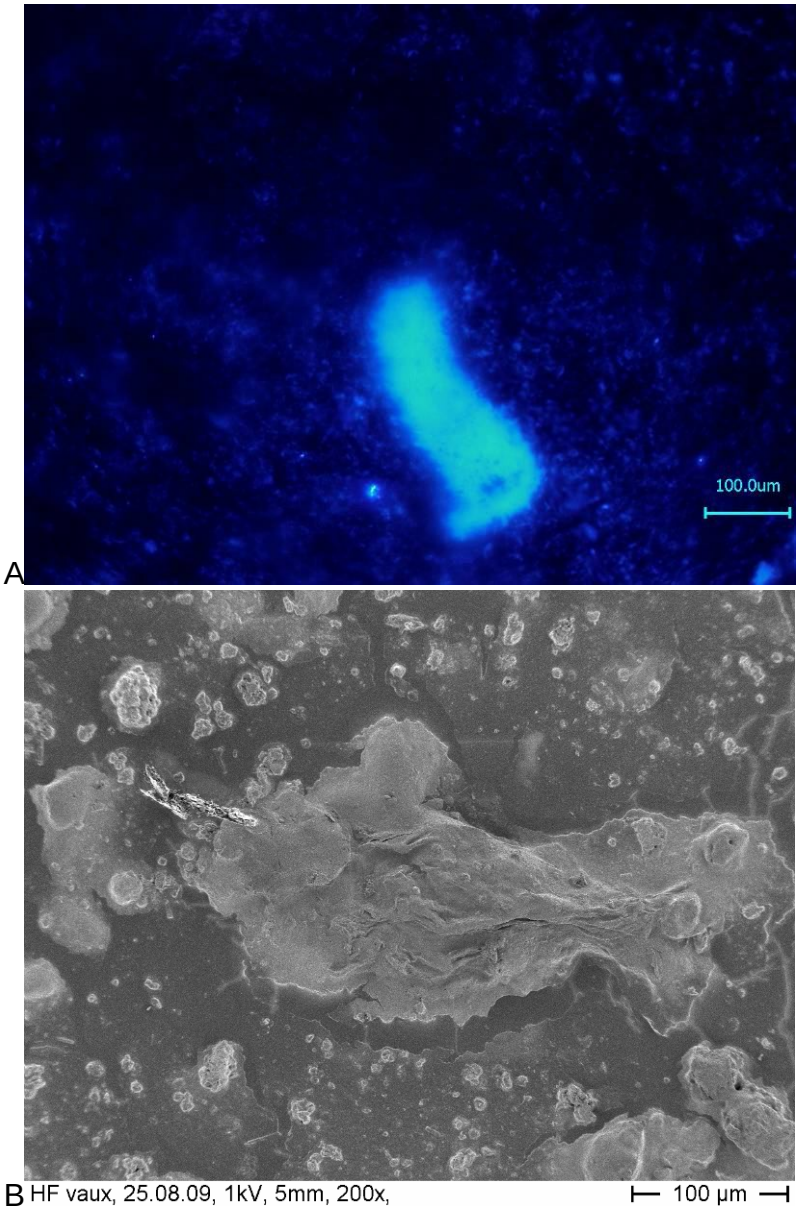

Figure S5. | Fluorescence spectrum of non-stained organic matrix (Fig. S8C) isolated from demineralized *V. gracilenta* fibers (green) is closely similar to those obtained for α-chitin (red).

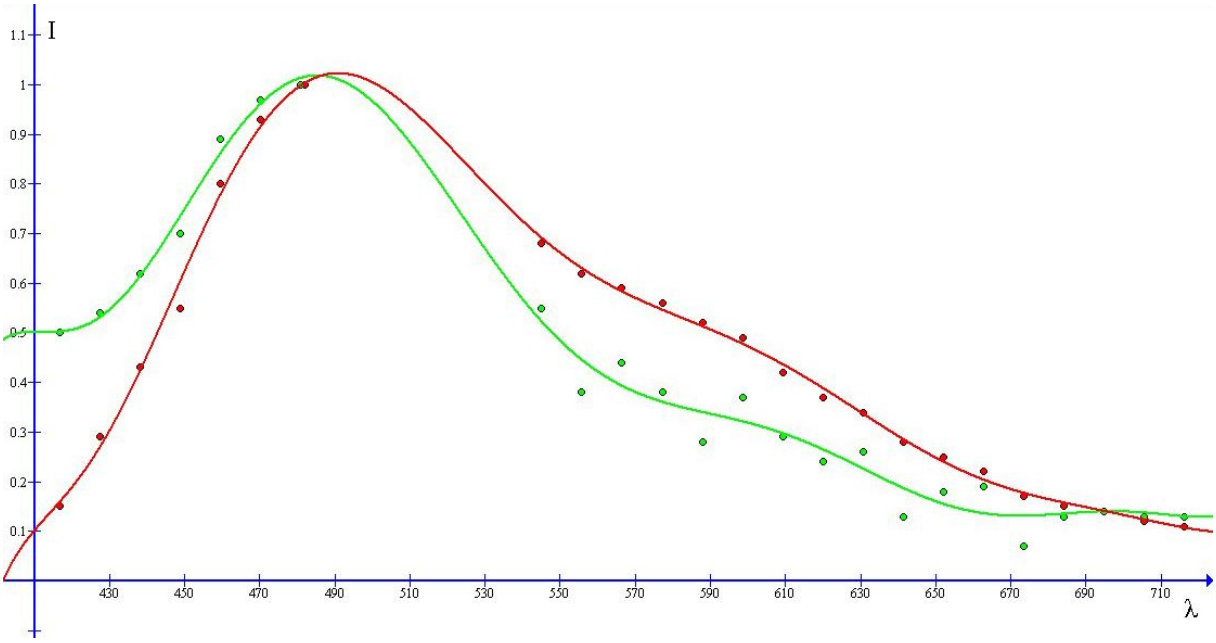

Figure S6. | Light (left) and fluorescence microscopy (right) images of the fragments isolated after HF-treatment of fossilized *V. gracilenta*. These fragments were analyzed using FTIR (results are represented above in supplementary results section) and after that stained with CFW. Light exposure time during fluorescence microscopy observations was 1/50 s.

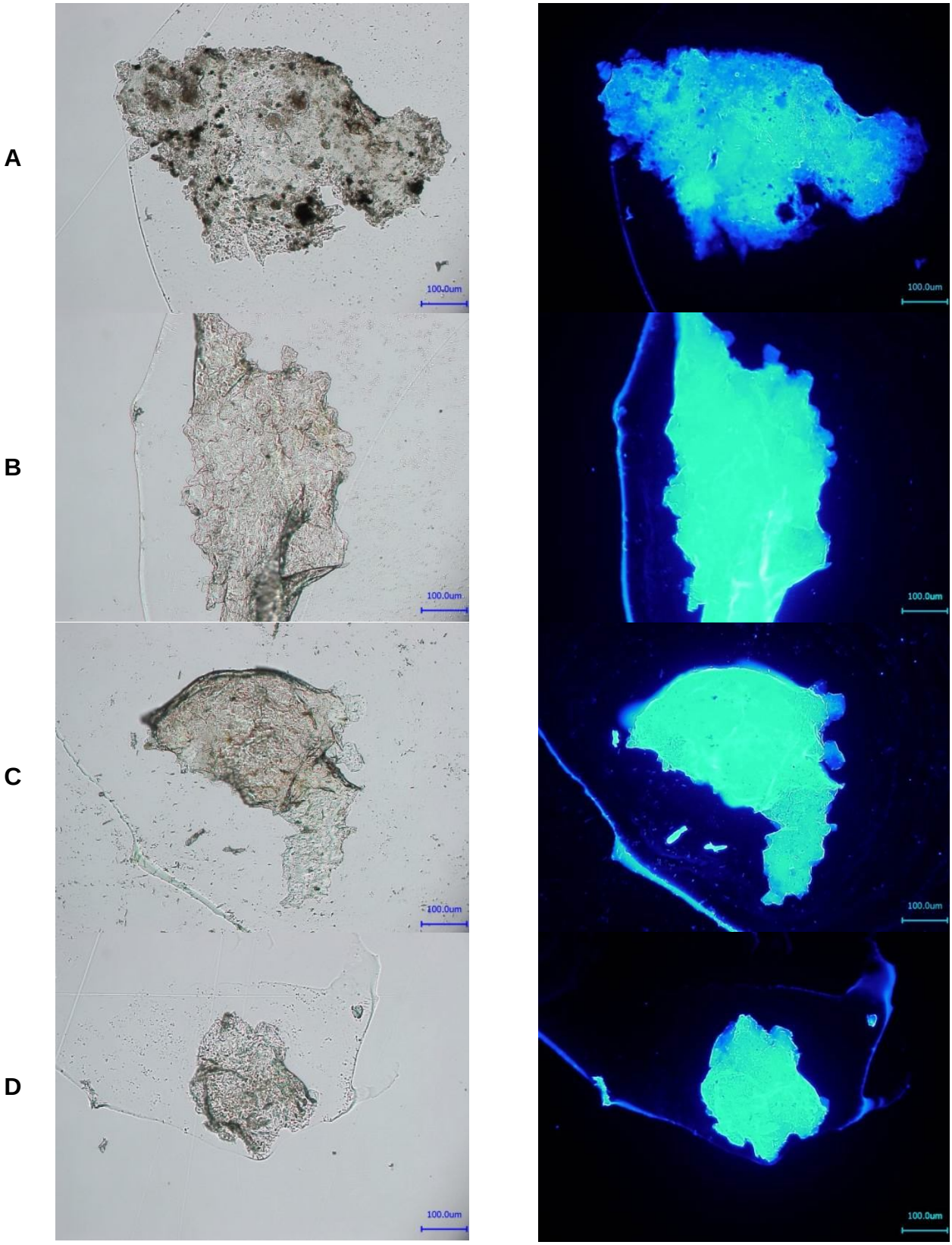

Figure S7. | TEM images (A, C) of the two different fragments of organic matrix isolated from *V. gracilenta* skeletal fibres demineralised using HF. Both fragments show nanofibrillar organization of the material. Electron diffraction patterns (B and C) of areas represented in A and C, respectively, confirm absence of any kind of crystalline mineral phase and showed, albeit weakly, an annular ring corresponding to the 2.59 Å and 3.56 Å spacing characteristic of α-chitin *(25, 26, 27)*.

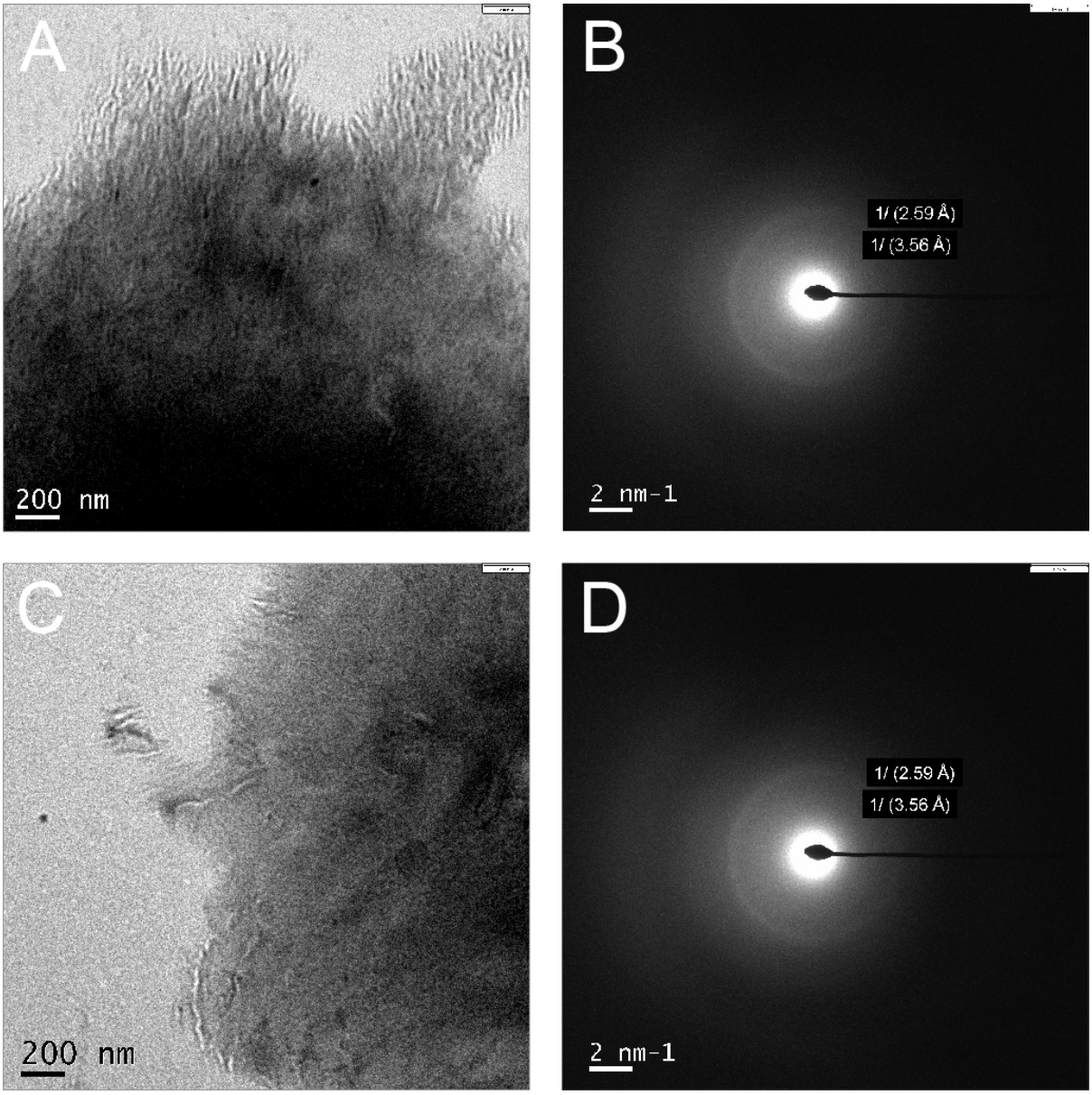

Figure S8. | Chitinase digestion. Light microscope (A, B) and fluorescence microscope (C, D) images of fibrous material isolated from fossilized remains of *V. gracilenta* after HF-treatment prior to the addition of chitinase solution (A, C) and after 8h insertion with chitinase (B, D). Light exposure time for fluorescence microscopy: 1/3 s.

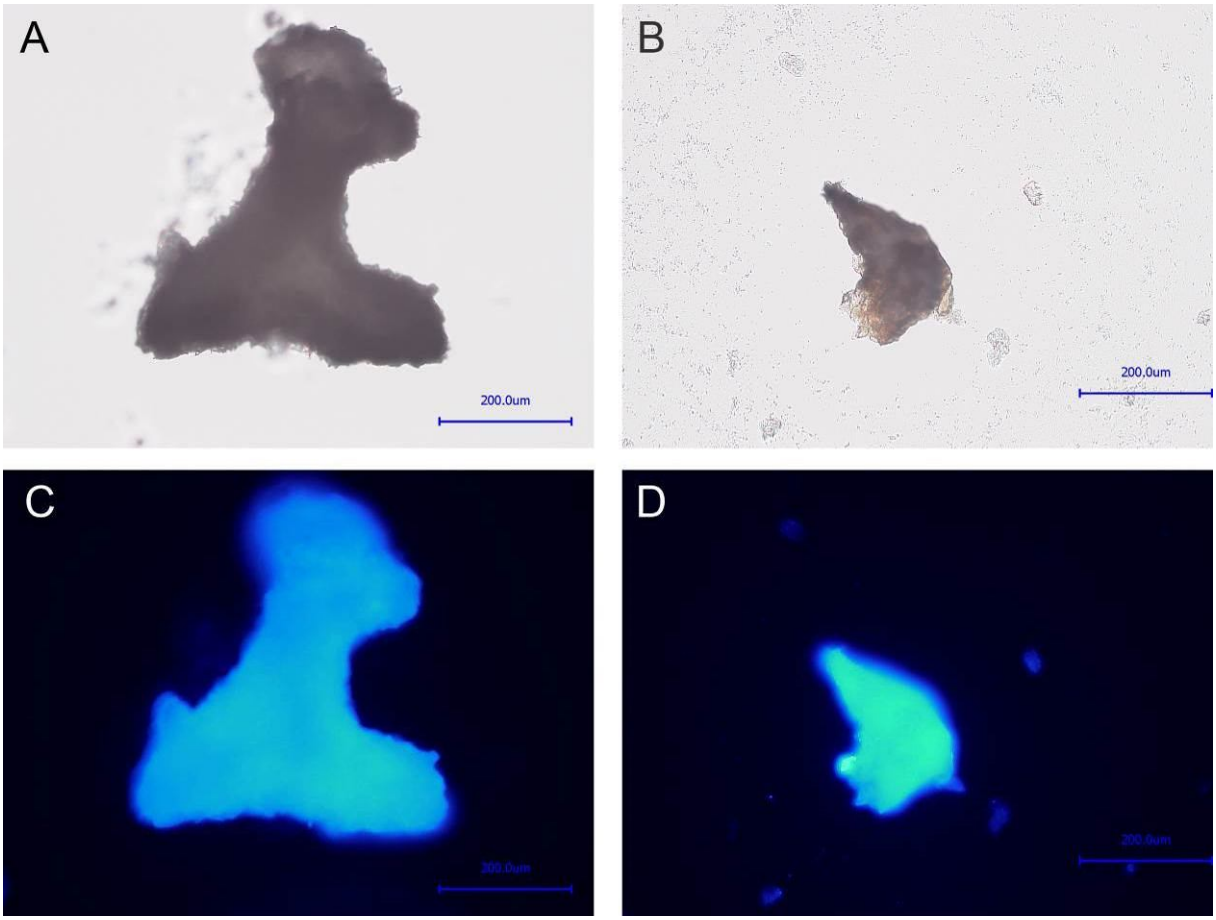

Figure S9. | SEM images of the cleaned brownish colored surface of fossilized *V. gracilenta* prior to HF-based treatment (A, B). Note the euhedral cubic crystals, partly with a pentagondodecahedral habit (B), which can be identified as pyrite *(24)* (see also Fig. S10).

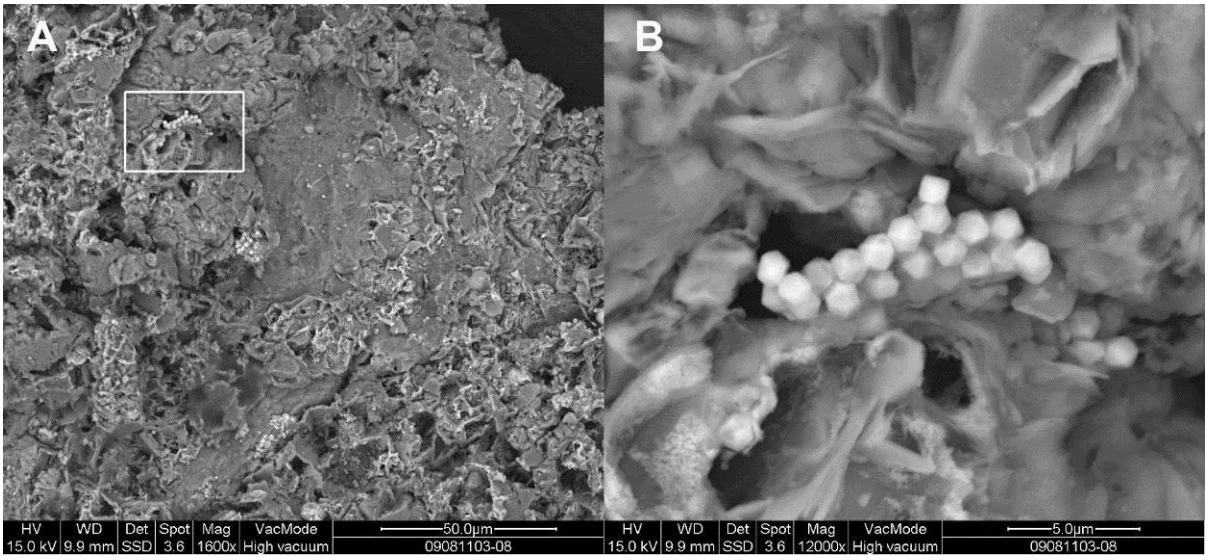

Figure S10. | Results of the EDX analysis carried out at 30kV of the cleaned surface of fossilized *V. gracilenta* represented in Fig. S9. The sample was not coated with carbon.

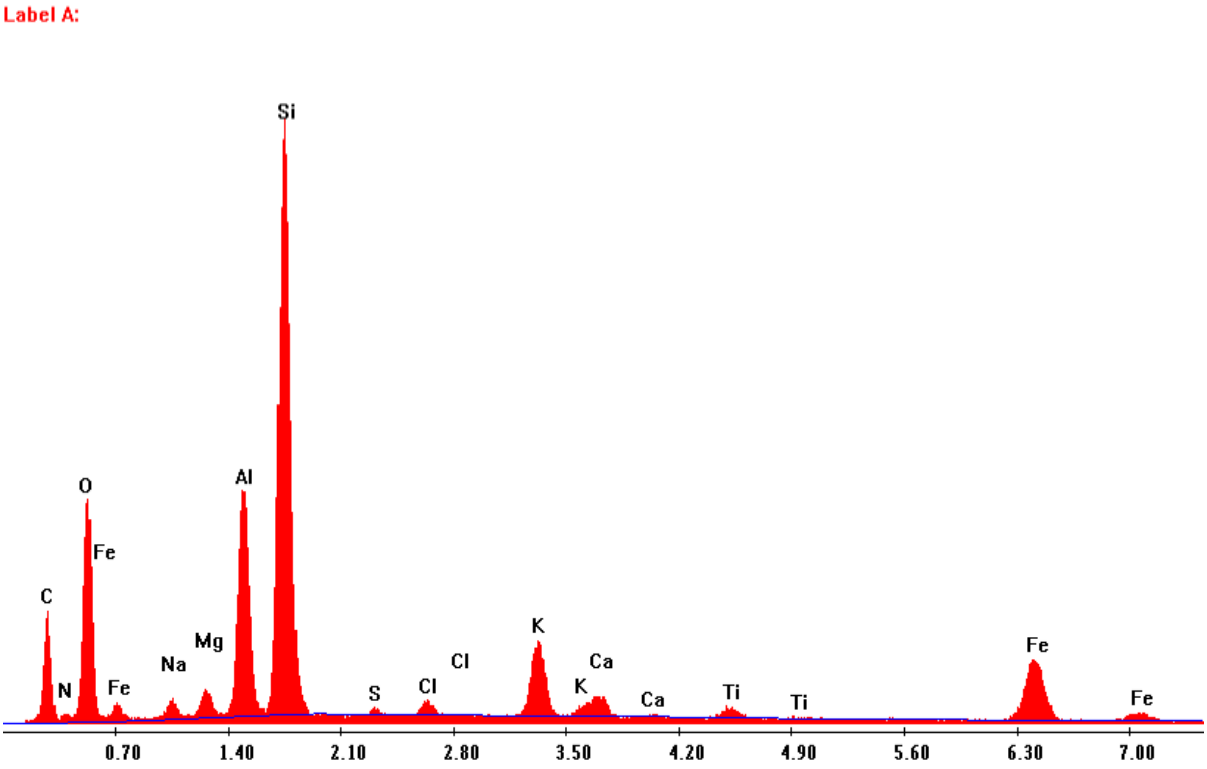

Figure S11. | HPLC chromatogram of D-glucosamine (DGlcN) (left) and the sample (right) (0.1 % TFA, H_2O/AcN linear gradient).

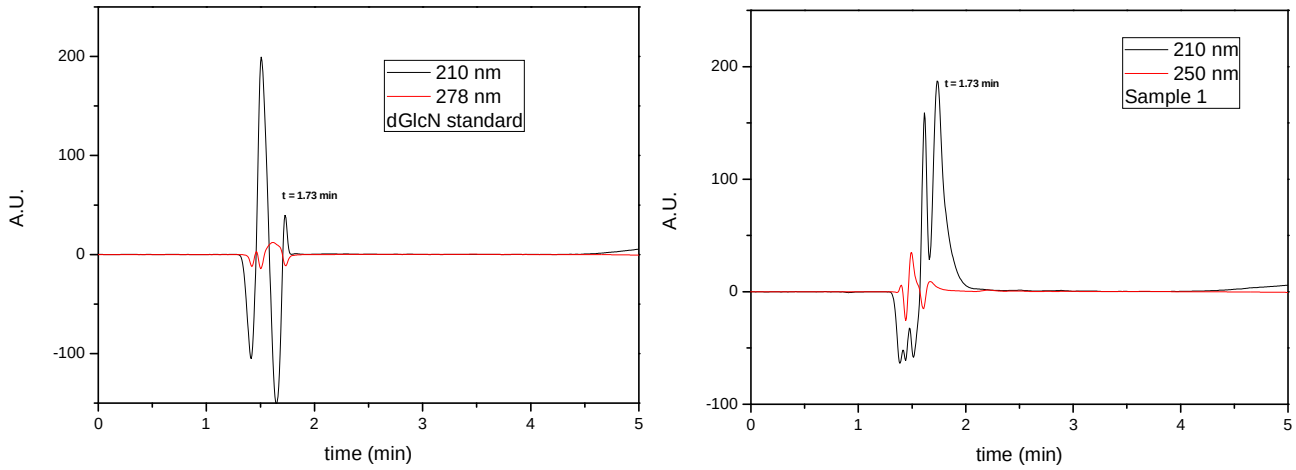

Figure S12. | HPSEC chromatogram of D-glucosamine (DGlcN) (left) and the sample (center) and the overlap the signals at 210 nm (right). (50 mM Phosphate buffer pH 7).

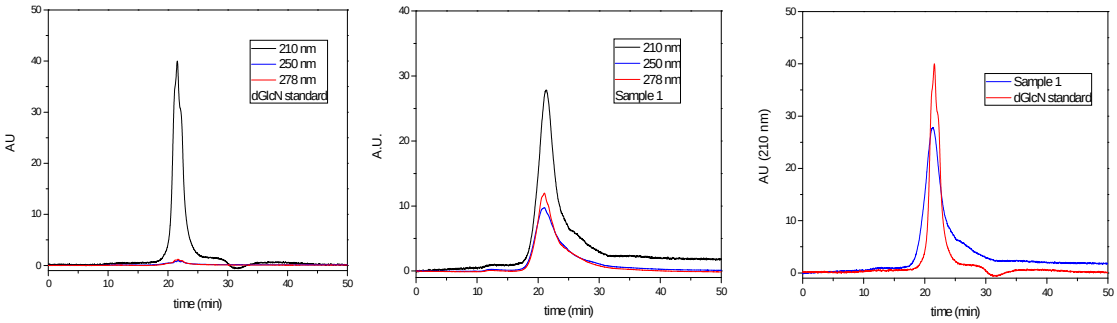

Figure S13. **|** HPCE chromatogram of D-glucosamine (DGlcN) (left) and the sample (right) (100 mM Sodium borate buffer, pH 8.3).

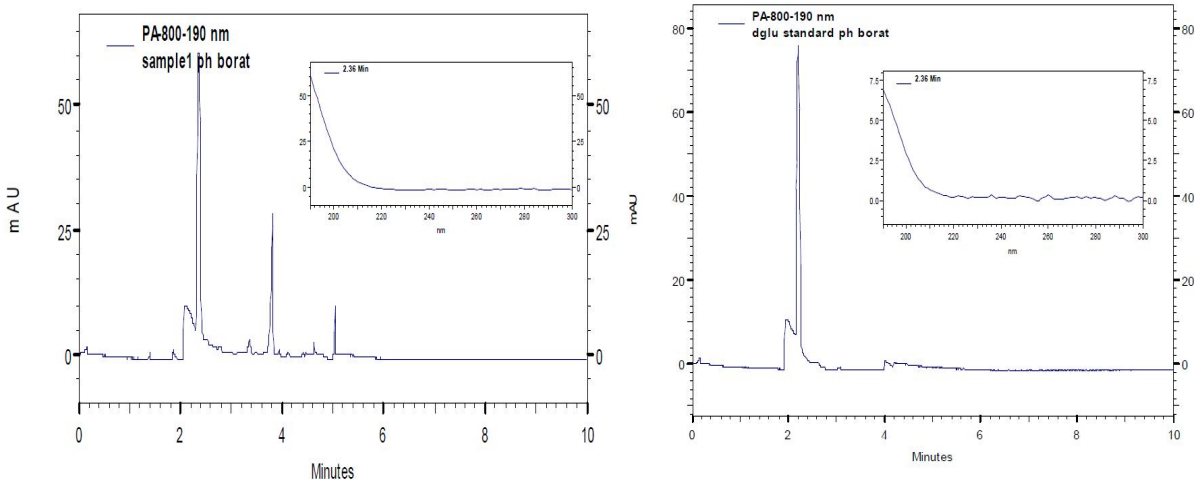

Figure S14. | ESI-MS of D-glucosamine (DGlcN) (left) and the sample (right).

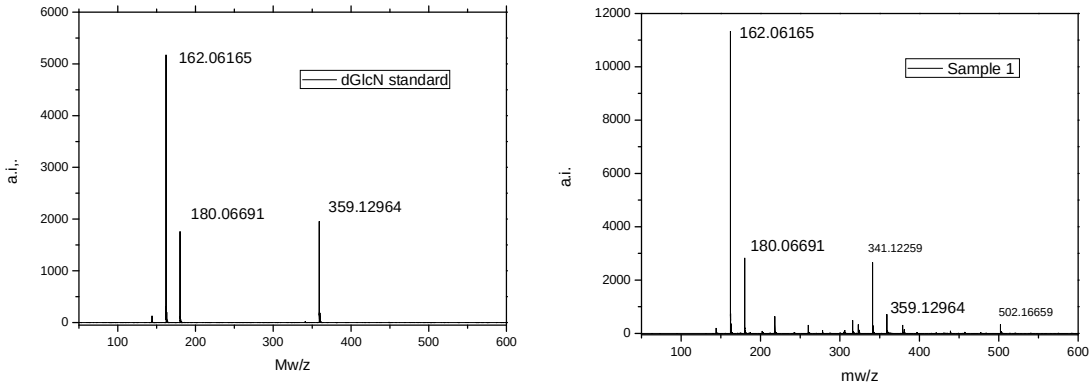

Figure S15. | TG curves (A and B) of *A. aerophoba* chitinous skeleton.

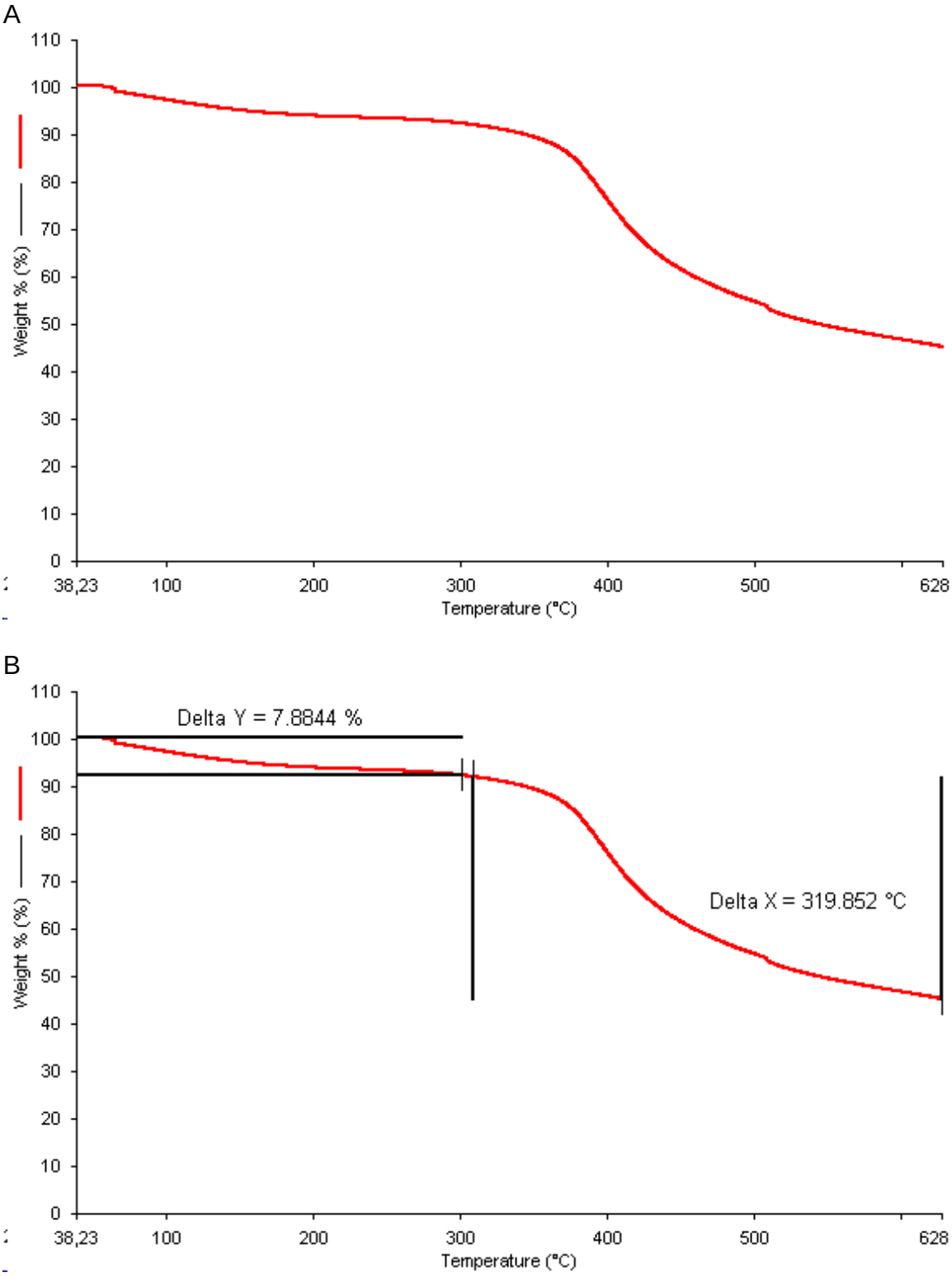

Figure S16. | Comparative FTIR spectra of the chitinous *A. aerophoba* sponge skeletons heated up to 300 ^{o}C (red line) and prior to heating (blue line).

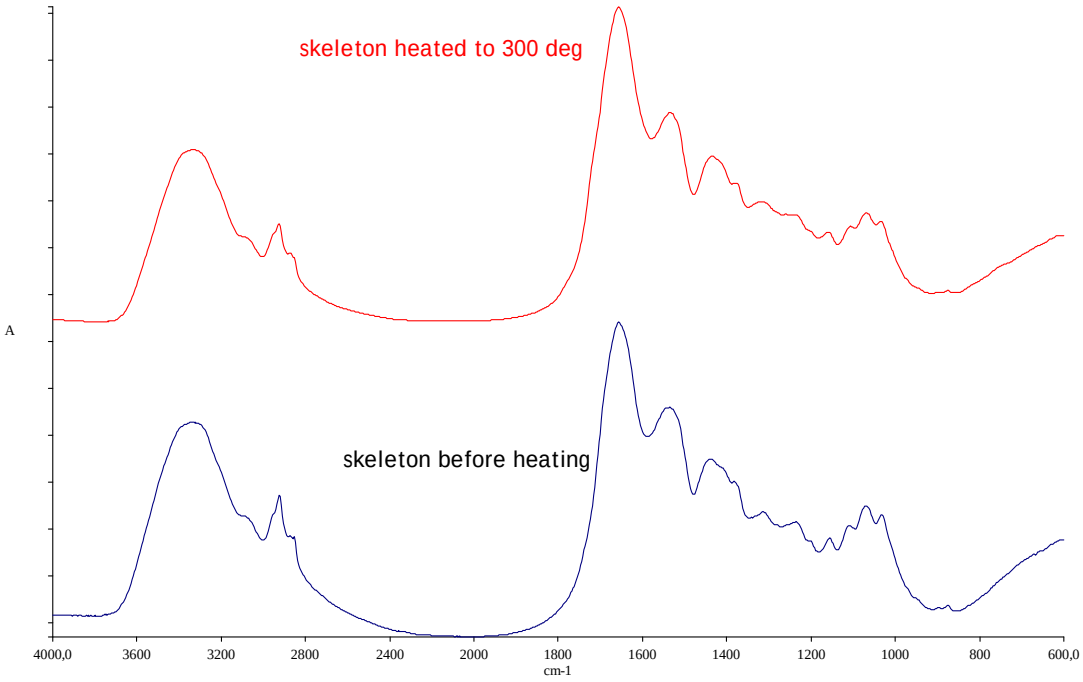

Figure S17. | Light (left) and fluorescence (right) microscopy images of the *I. basta* chitinous skeleton sample heated at 300°C, cleaned using 3M HCl and stained after that with CFW. Light exposure time: 1/10 s.

Figure S18. | Light (left) and fluorescence (right) microscopy images of another part of the same sample which was cleaned using HF and stained after that with CFW. Light exposure time: 1/50s.

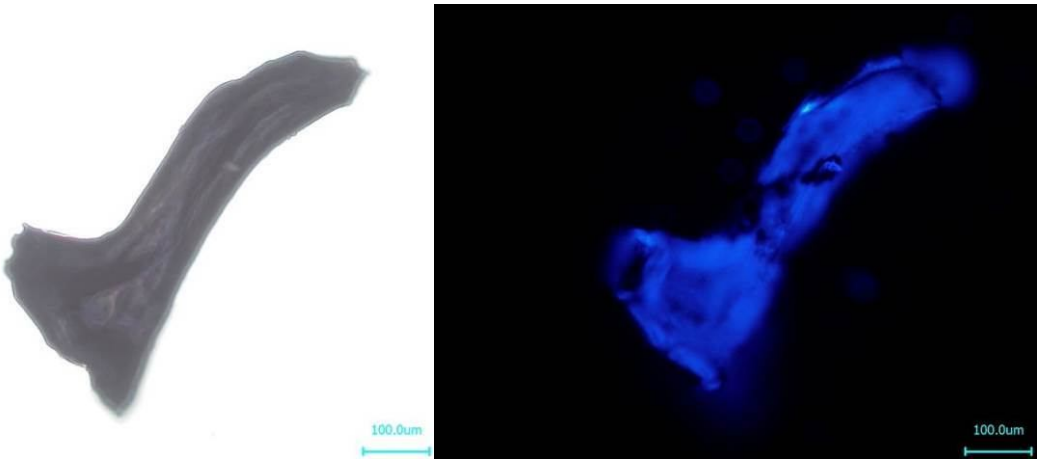

Figure S19. **|** Light (left) and fluorescence (right) microscopy images of the thermal untreated *I*. *basta* sponge skeleton stained with CFW. Light exposure time: 1/50s.

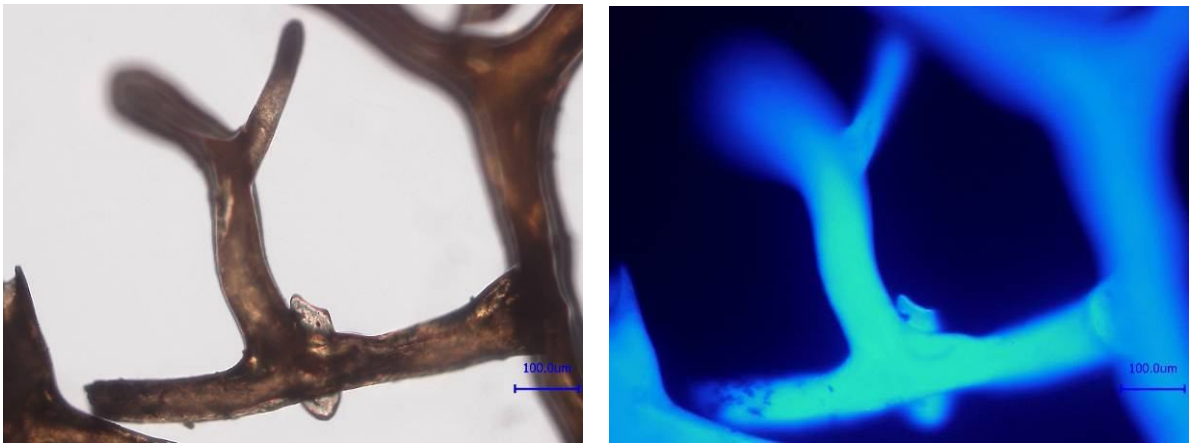

Figure S20. | Conversion of the measured ^{14}C concentration 0.0057 ± 0.0009 fraction modern into calendar years with the program OxCal V4.2.3 (*35*). As calibration curve the IntCal13 (*36*) for the northern hemisphere was used. The red, blue, and grey curves show the measured concentration (in conventional years), the calibration curve, and the probability density for the calendar years, respectively.

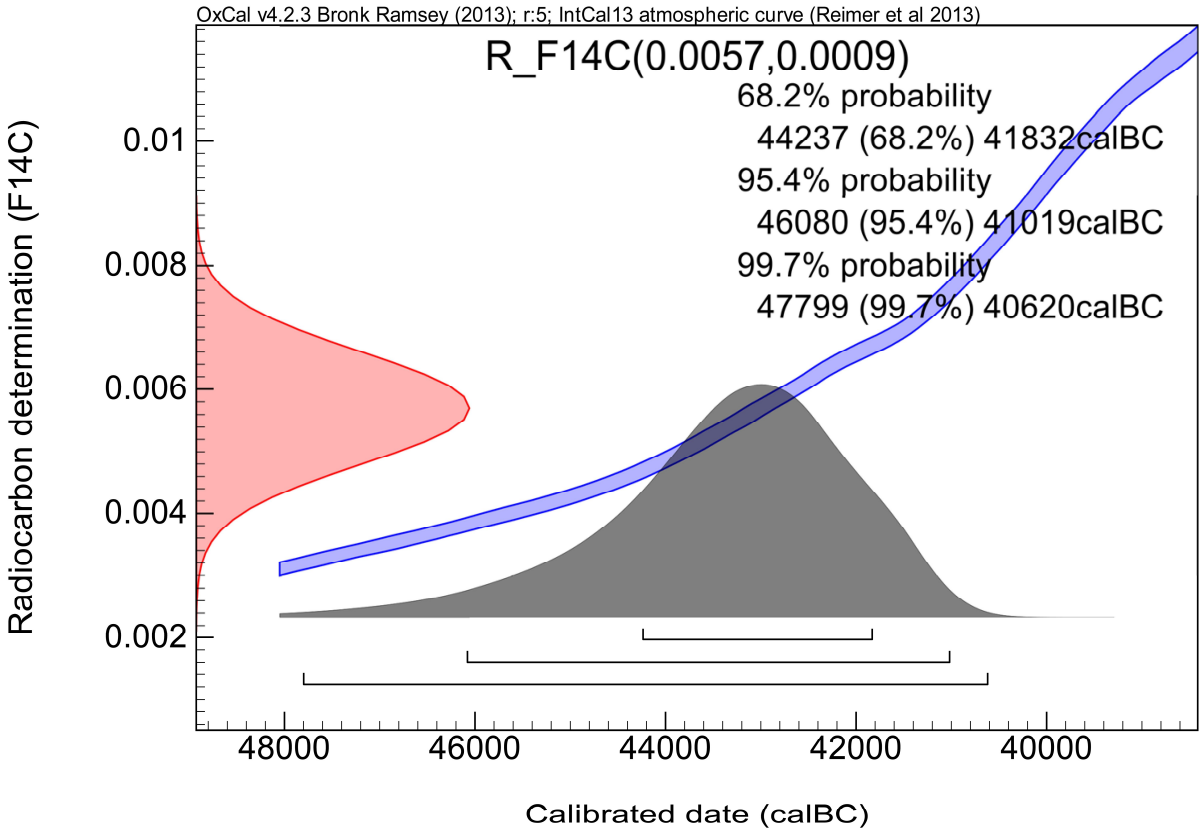

Figure S21. | Fluorescence microscopy image of the surface of *V. gracilenta* fossil stained with Bisbenzimide H 33342 shows no evidence of the presence of some DNA remains.

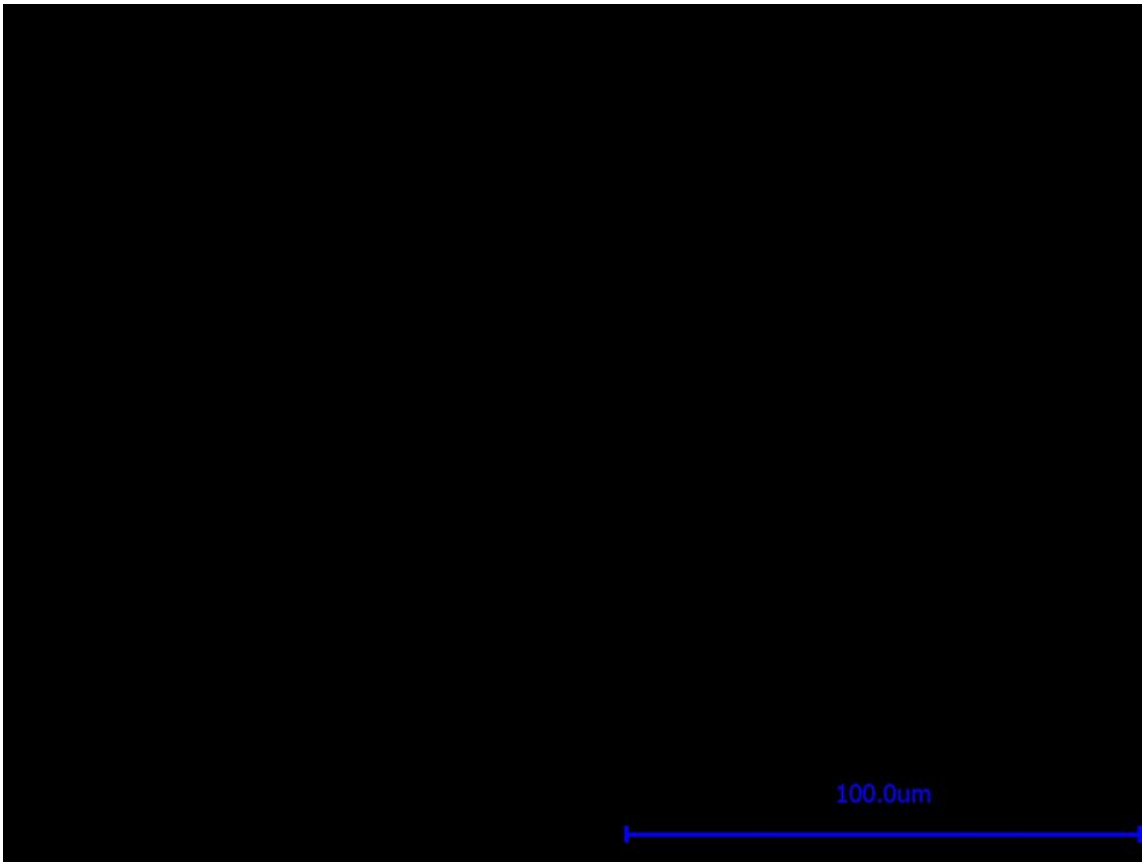

Figure S.22. | ESI-MS spectra of the rock in the close proximately to the *Vauxia gracilenta* sponges remains.

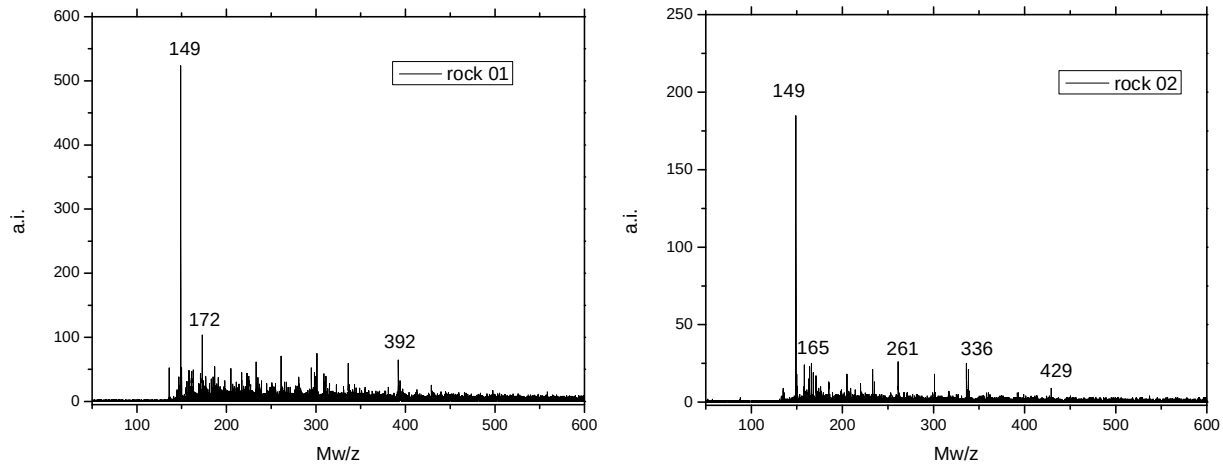

Figure S23. | ESI-MS spectra of pure MeOH (LC-MS grade).

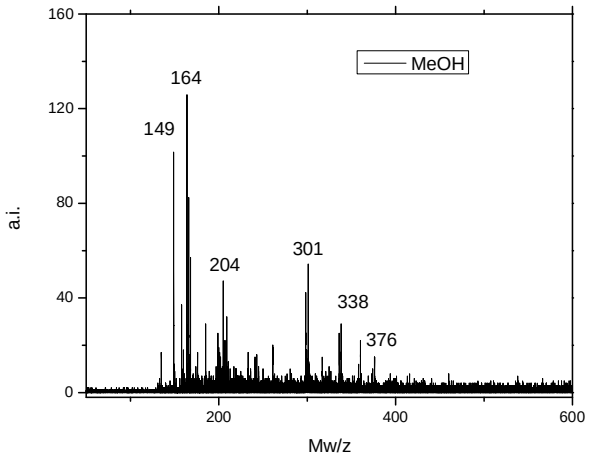

SI References

1. Aguilar, M. I. HPLC of peptides and proteins; In: *Methods in Molecular Biology,* (ed. Aguilar, M.-I.), **251,** pp. 3-9, Totowa (NJ, USA): Humana Press, (2004).

2. Mant, C. T., Chao, H., Hodges, R. S. Effect of mobile phase on the oligomerization state of α-helical coiled-coil peptides during high-performance size-exclusion chromatography. *J. Chromatogr, A* **791,** 85-98 (1997).

3. Mant, C. T., Parker, J. M. R., Hodges, R. S. Size-exclusion high-performance liquid chromatography of peptides. Requirement for peptide standards to monitor column performance and non-ideal behaviour. *J. Chromatogr.* **397,** 99-112 (1987).

4. Brown, P. R., Grushka E., Lunte S. *Advances in Chromatography* **43,** New York (USA): Marcel Dekker, (2005).

5. Mohacek-Grosev, V., Bozac, R., Puppels G. J. Vibrational spectroscopic characterization of wild growing mushrooms and toadstools. *Spectrochim. Acta Part A* **57,** 2815–2829 (2001).

6. Cardenas, G., Cabrera, G., Taboada, E., Miranda, P.S. Chitin characterization by SEM, FTIR, XRD, and ^{13}C cross polarization/mass angle spinning NMR. *J. Appl. Polymer Sci.* **93(4),** 1876-1885 (2004).

7. Yamaguchi, Y., Nge, T. T., Takemura, A., Hori N., Ono H. Characterization of uniaxially aligned chitin film by 2D FT-IR spectroscopy. *Biomacromolecules* **6(4),** 1941-1947 (2005).

8. Pearson, F.G., Marchessault, R.H., Liang, C.Y. Infrared Spectra of Crystalline Polysaccharides.V. Chitin. *J. Polym. Sci.* **113,** 101-116 (1960).

9. Seoudi, R., Nada, A. M. A., Abd Elmongy, S., Hamed S. S. Fourier Transform Infrared Spectroscopic and AC Electrical Conductivity Studies of Chitin and Its Derivates. *J. Appl. Polym. Sci.* **98,** 936-943 (2005).

10. Lavall, R. L., Assis, O. B. G., Campana-Filho, S. P. α-Chitin from the pens of *Loligo* sp.: Extraction and characterization. *Biores. Technol.* **98(13),** 2465-2472 (2007).

11. Paulino, A. T., Simionato, J. I., Garcia, J. C., Nozaki, J. Characterization of chitosan and chitin produced from silkworm chrysalides. *Carboh. Pol.* **64,** 98–103 (2006).

12. Majtan, J., et al. Isolation and characterization of chitin from bumblebee (*Bombus terrestris*). *Inter. J.Biol. Macromol.* **40(3),** 237-241 (2007).

13. Crespo, M.O., Martínez, M. V., Hernández, J. L., Lage Yusty, M. A. High-performance liquid chromatographic determination of chitin in the snow crab, *Chionoecetes opilio. J. Chromat. A* **1116,** 189–192 (2006).

14. Watt, D. K., Yorke, S. C., Slim, G. C. Comparison of ovine, bovine and porcine mucosal heparins and low molecular weight heparins by disaccharide analyses and ^{13}C NMR*. Carboh. Pol.* **33,** 5-11 (1997).

15. Berth, G., Voigt, A., Dautzenberg, H., Donath, E., Möhwald, H. Polyelectrolyte Complexes and Layer-by-Layer Capsules from Chitosan/Chitosan Sulfate. *Biomacromol.* **3(3),** 579–590 (2002).

16. El Rassi, Z. (ed.) *Carbohydrate Analysis: High Performance Liquid Chromatography and Capillary Electrophoresis*. Amsterdam (Netherlands): Elsevier Science, (1995).

17. Grimshaw, J., et al. Quantitative analysis of hyaluronan in vitreous humor using capillary electrophoresis. *Electrophoresis* **15,** 936-940 (1994).

18. Malsch, R., Harenberg, J., Heene, D. L. High-resolution capillary electrophoresis and polycrylamide gel electrophoresis of heparins. *J. Chromat. A* **716,** 259-268 (1995).

19. Damm, J. B. L., Overklift, G. T. Indirect UV detection as a non-selective detection method in the qualitative and quantitative analysis of heparin fragments by high-performance capillary electrophoresis. *J. Chromat. A* **678,** 151-165 (1994).

20. Banoub, J., et al. *In situ* formation of C-glycosides during electrospray ionization tandem mass spectrometry of a series of synthetic amphiphilic cholesteryl polyethoxy neoglycolipids containing N-acetyl-D-glucosamine. *J. Am. Soc. Mass Spectr.* **16,** 565-570 (2005).

21. Hsu, J., Chang, S. J., Fran, A. H. MALDI-TOF and ESI-MS analysis of oligosaccharides labeled with a new multifunctional oligosaccharide tag. *J. Am. Soc. Mass Spectr.* **17,** 194-204 (2006).

22. Yao, Y.-Y., et al. Structural simulation and protein engineering to convert an endo-chitosanase to an exo-chitosanase. *Protein Engineering, Design & Selection* **21(9),** 561–566 (2008).

23. Stach, S. *Polysaccharide aus marinen Bakterien und der Mikroalge Chlorella vulgaris.* Göttingen (Germany): Cuvillier (2005).

24. Martin-Gonzales, A., Wierzchos, J., Gutierrez, J-C., Alonso, J., Ascaso, C. Double fossilization in eukaryotic microorganisms from Lower Cretaceous amber. *BMC Biology* **7,** 9, doi: 10.1186/1741-7007-7-9 (2009).

25. Minke, R., Blackwell, J. The structure of α-chitin. *J. Mol. Biol.* **120,** 167-181 (1978).

26. Dweltz, N.E. The structure of chitin. *Biochim. Bioph. Acta* **44,** 416-435 (1960).

27. Machado, J., Reis, M.L., Coimbra, J., Sa, C. J. Studies on chitin and calcification in the inner layers of the shell of *Anodonta cygnea*. *J. Comp. Physiol. B* **161,** 413-418 (1991).

28. Steinhof, A., Adamiec, G., Gleixner, G., van Klinken, G. J., Wagner, T. The new ^{14}C analysis laboratory in Jena, Germany. *Radiocarbon* **46,** 51-58 (2004).

29. Steinhof, A., Hejja, I., Wagner, T. Improvements of the Jena AMS system, *Nuclear Instruments and Methods B* **268,** 902-905 (2010).

30. Brunner, E. et al. Chitin-based scaffolds are an integral part of the skeleton of the marine demosponge *Ianthella basta*. *J. Struct. Biol.* **168,** 539-547 (2009).

31. Ehrlich, H. et al. First evidence of chitin as a component of the skeletal fibers of marine sponges. Part I. Verongidae (Demospongia: Porifera), *J. Exp. Zool. (Mol Dev Evol)* **308B,** 347-356 (2007).

32. Ehrlich, H., et al. Three dimensional chitin-based scaffolds from Verongida sponges (Demospongiae: Porifera). Part I. Isolation and Identification of Chitin. *Int. J. Biol. Macromol.* **47,** 132-140 (2010).

33. Lowe, D-C. Problems associated with the use of coal as a source of ^{14}C free background material. *Radiocarbon* **31,** 117-120 (1989).

34. Wattel-Koekkoek, E. J. W., van Genuchten, P. P. L., Buurman, P., van Lagen, B. Amount and composition of clay-associated soil organic matter in a range of kaolinitic and smectitic soils. *Geoderma* **99,** 27-49 (2001).

35. Ramsey, B. C. Bayesian analysis of radiacarbon dates. *Radiocarbon* **51,** 337-360 (2009).

36. Reimer, P. J., et al. IntCal13 and Marine13 Radiocarbon Age Calibration Curves 0-50,000 Years cal BP. *Radiocarbon* **55**, 1869–1887 (2013).

37. Oskam, C. L., et al Fossil avian eggshell preserves ancient DNA. *Proc. R. Soc. B* **277,** 1991-2000, doi: 10.1098/rspb.2009.2019 (2009).

38. Barton, H. A., Taylor, N. M., Lubbers, B. R., Pemberton, A. C. DNA extraction from low-biomass carbonate rock: An improved method with reduced contamination and the low-biomass contaminant database. *J. Microbiol. Meth.* **66,** 21–31 (2006).